IEEE Access
Multidisciplinary | Rapid Review | Open Access Journal

Received June 25, 2019, accepted July 1, 2019, date of publication July 8, 2019, date of current version July 25, 2019.

Digital Object Identifier 10.1109/ACCESS.2019.2927159

A Feature Set for Structural Characterization of Sphere Gaps and the Breakdown Voltage Prediction by PSO-Optimized Support Vector Classifier

ZHIBIN QIU[1], (Member, IEEE), AND XUEZONG WANG[2]
[1]Department of Energy and Electrical Engineering, Nanchang University, Nanchang 330031, China
[2]School of Electrical Engineering and Automation, Wuhan University, Wuhan 430072, China

Corresponding author: Zhibin Qiu (qiuzb@ncu.edu.cn)

This work was supported in part by the China Postdoctoral Science Foundation under Grant 2016M602354, and in part by the Fundamental Research Funds for the Central Universities under Grant 2042018kf0020.

ABSTRACT Air insulation strength relates closely to the electrostatic field distribution of the gap configuration. To achieve insulation prediction on the basis of electric field (EF) simulations, the spatial structure is characterized by a feature set including 38 parameters defined on a straight line between sphere electrodes. A support vector classifier (SVC) with particle swarm optimization (PSO) is used to establish a prediction model, whose input variables are those features. The EF nonuniform coefficient f of each sample gap is calculated and used for training sample selection according to the ranges of f values. Trained by only 11-sample data, the PSO-optimized SVC model is employed to predict the power frequency breakdown voltages of 260-sphere gaps with a wide range of structure sizes. The predicted values coincide with the standard data given in IEC 60052 very well, with the same trend and minor relative errors. The MAPEs of the five predictions with different training sets are within 2.0%. The model is also effective to predict the breakdown voltages of Φ9.75-cm sphere–Φ6.5-cm sphere gaps, whose MAPEs are within 2.6%. The results demonstrate the effectiveness of the EF feature set and the generalization ability of the SVC model under the case of limited samples. This paper lays the foundation for estimating the dielectric strength of other air gaps with similar structures.

INDEX TERMS Breakdown voltage prediction, sphere gap, electric field features, shortest interelectrode path, support vector classifier (SVC), particle swarm optimization (PSO).

I. INTRODUCTION

Air is the most commonly used dielectric in electric power systems, and its strength is of vital importance for insulation design of many electrical equipment. The withstand voltages of air-insulated gaps, with various electrode structures and gap spacings, have always been investigated by experiments. Since the discharge theory is still not yet perfect, the reliability of an insulation structure should be verified by full-scale discharge tests. In order to provide theoretical guidance and methodology for electrical insulation design, it is necessary to predict air gap breakdown voltage accurately.

Classical gas discharge theories including the Townsend theory [1] and the streamer theory [2], [3] are beneficial to explain air discharge phenomena theoretically. Their interpretations of the discharge process have some differences and are applicable for different cases, but the common ground is that air gap breakdown results from out-of-limit of the electric field (EF) applied on the air dielectric. Some streamer inception criteria, like the critical charge criterion [2], [4] and the inception field strength criterion [5], [6], have been used to calculate air gap breakdown voltages. These criteria usually consider the EF distribution and field intensity in the vicinity of the high voltage (HV) electrode, and take the critical space charge number or the critical field strength as the criterion to judge streamer inception or gap breakdown. However, the related studies were carried out on specific electrode

The associate editor coordinating the review of this manuscript and approving it for publication was Lei Zhao.

systems and some key physical parameters are applicable to limited cases. It is still unclear whether these criteria are suitable for various gap arrangements [7]. Therefore, some new approaches are expected to be put forward to solve this problem.

Air discharge process is so complex that it is difficult to be described by some deterministic governing equations. Especially for air gaps with large spacings, the discharge process is usually with random trajectory. On account of this, the gap discharge is considered as a grey correlation problem, while the external influencing factors and the breakdown voltage are respectively the inputs and the output, and the physical process during the discharge is viewed as a grey box. The key problems that need to be solved for air gap breakdown voltage prediction are how to parameterize the influencing factors and how to describe the grey relations between those factors and the air gap strength.

The macro influencing factors on the air gap strength include the applied voltage shape and polarity, the gap configuration, and the atmospheric conditions [8], [9]. When an air gap is submitted to a steady voltage, e.g., the power frequency AC voltage, and under a constant atmospheric environment, the decisive factor is the gap structure, which may be parameterized by some electrostatic field features [10]. On the other hand, some artificial intelligence algorithms are useful to describe the relations between the influencing factors and the breakdown voltage. For example, the artificial neural network (ANN) [11], [12], the support vector machine (SVM) [13]–[15] and the fuzzy logic [16], [17] have already been used by some researchers to predict the external insulation strength. These achievements preliminarily verify the feasibility of air insulation prediction by some mathematical algorithms, but many interesting topics are still worthy to be studied in detail.

In this paper, an EF feature set is used for structural characterization of sphere gaps, which is defined on a straight line between sphere electrodes. A support vector classifier (SVC) model, taking the EF features as input variables, is applied for breakdown voltage prediction of sphere gaps with different structure sizes. A prediction of power frequency breakdown voltages of sphere gaps is performed and a comparison with the test values provided in IEC 60052 [18] verifies the rationality of the proposed feature set and the availability of the prediction method. This study is beneficial to provide reference for numerical simulation and intelligent prediction research of air gap discharge characteristics.

II. ELECTRIC FIELD FEATURE SET ON THE SHORTEST INTERELECTRODE PATH

In previous studies [10], [14], [15], the features used for structural characterization of air gaps were defined in the whole computational area and the hypothetic discharge channel, on the HV electrode surface and along the shortest discharge path. The spatial regions were divided into four categories according to volume, area and line. But the features belong to the types of volume and area are not easy to be extracted

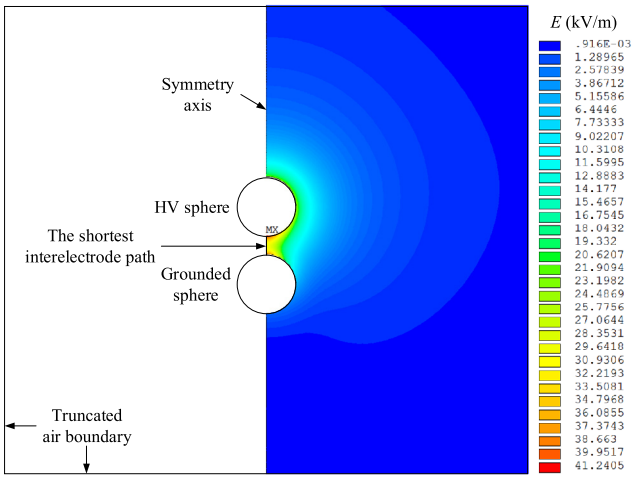

FIGURE 1. A sphere gap simulation model and the EF calculation result with $D = 10$ cm and $d = 3$ cm.

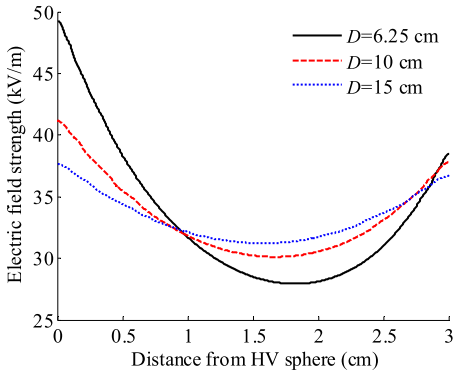

FIGURE 2. EF distribution along the interelectrode path of 3 cm sphere gaps with $D = 6.25$, 10 and 15 cm.

for gap configurations with atypical or complex electrodes. Here in this paper, a new feature set is extracted only on an interelectrode path, thus to map the three-dimensional EF distribution to a one-dimensional straight line. The sphere gap is taken as the research object, and the electrostatic field distribution is simulated by the finite element method (FEM) for EF feature definition and extraction.

A. ELECTROSTATIC FIELD CALCULATION

The sphere gap is with axisymmetric structure, and therefore a two-dimensional axisymmetric model can be used for EF simulation. A unit voltage $U = 1$ kV was applied on the HV sphere, and the grounded sphere was applied zero potential. A truncated boundary was set at the outer air layer. A simulation model and the EF calculation result of a sphere gap with $D = 10$ cm and $d = 3$ cm are shown in Figure 1. D is the sphere diameter and d is the gap spacing. The maximum EF intensity E_{max} appears at the tip of the HV sphere.

The values of the EF strength were extracted on some equidistant sampling points along the interelectrode path, so as to plot the EF distribution curve. Taking the 3 cm sphere gaps with $D = 6.25$, 10 and 15 cm as examples, the E-d curves are shown in Figure 2, which are

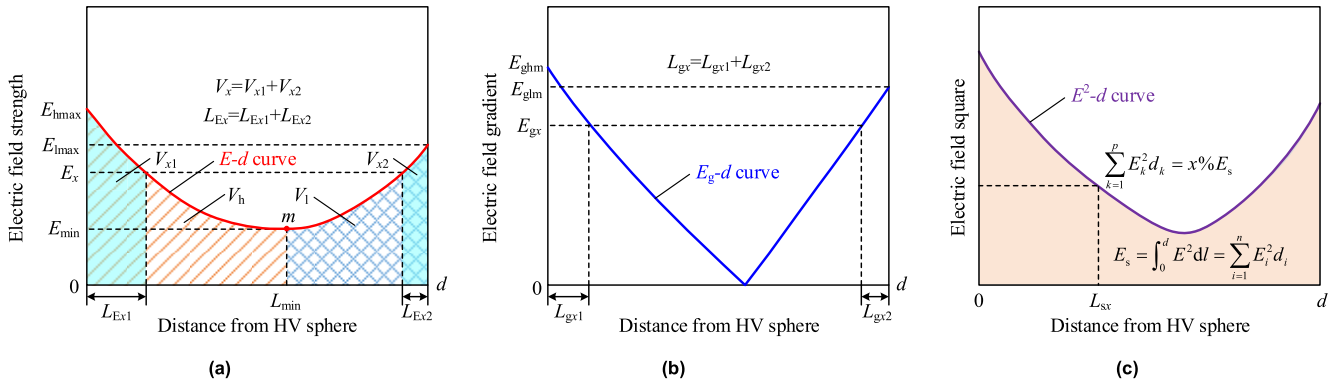

FIGURE 3. Schematic diagrams of the EF intensity, gradient and EF square along the sphere gap interelectrode path. (a) E-d curve, (b) E_g-d curve, and (c) E^2-d curve.

U-shaped curves. Two maximum values appear on both sides of the interelectrode path. Under the same gap spacing, the value of E_{max} decreases with a larger sphere diameter. Taking the point with the minimum EF strength as the critical point, the E-d curve can be divided into the HV side and the low voltage (LV) side. In view of the U-shaped EF distribution curve, the following feature set was used to parameterize the structure of the sphere gap.

B. EF FEATURES FOR STRUCTURAL CHARACTERIZATION

The feature set used for structural characterization of sphere gaps can be divided into 6 groups, including the EF intensity E, EF gradient E_g, EF square E^2, EF integral V, path length L, and EF inhomogeneity. The schematic diagrams of the E-d, E_g-d and E^2-d curves are shown in Figure 3.

(1) EF intensity, including the six features defined as (1) and (2), where m is the serial number of the point with the minimum EF intensity, n is the amount of these sampling points, and E_i, E_j, E_k are the EF intensity of the ith, jth and kth sampling point. E_{hmax} and E_{lmax} are the maximum field intensity respectively at the HV and LV side of the shortest interelectrode path. E_{min} and E_a are the minimum and average field strength. E_{std2} and E_{std} are the variance and standard deviation of the EF intensity on this path. E_{hmax}, E_{lmax} and E_{min} are shown in Figure 3(a).

$$\begin{cases} E_{hmax} = \max E_i \quad (i = 1, 2, \cdots, m) \\ E_{lmax} = \max E_j \quad (j = m+1, m+2, \cdots, n) \\ E_{min} = \min E_k \quad (k = 1, 2, \cdots, n) \\ E_a = \sum_{k=1}^{n} E_k / n \end{cases} \tag{1}$$

$$\begin{cases} E_{std2} = \frac{1}{n}\sum_{k=1}^{n}(E_k - E_a)^2 = \frac{1}{n}\sum_{k=1}^{n} E_k^2 - E_a^2 \\ E_{std} = \sqrt{E_{std2}} = \sqrt{\frac{1}{n}\sum_{k=1}^{n} E_k^2 - E_a^2} \end{cases} \tag{2}$$

(2) EF gradient, including the three features defined in (3). E_{ghm} and E_{glm} are the maximum values of the EF gradient respectively at the HV and LV side, as shown in Figure 3(b), and E_{ga} is the average value.

$$\begin{cases} E_{ghm} = \max(|-\text{grad}E_i|) \quad (i = 1, 2, \cdots, m) \\ E_{glm} = \max(|-\text{grad}E_j|) \quad (j = m+1, m+2, \cdots, n) \\ E_{ga} = \sum_{k=1}^{n} (|-\text{grad}E_k|)/n \end{cases} \tag{3}$$

(3) EF square, including two features as (4), where $d_k = d/(n-1)$, and it is the distance between two neighboring points. E_s is the integral of E^2, which is the envelope area between the coordinate axis and the E^2-d curve, as shown in Figure 3(c). E_{sa} is the expected value of E_s.

$$\begin{cases} E_s = \int_0^d E^2 dl \approx \sum_{k=1}^{n} E_k^2 d_k \\ E_{sa} = \frac{E_s}{d} \approx \frac{1}{n}\sum_{k=1}^{n} E_k^2 \end{cases} \tag{4}$$

(4) EF integral, including V_x, V_h and V_l, which are defined as (5) and shown in Figure 3(a). V_x is the integral on the path where the EF intensity $E > E_x = x\%E_{hmax}$, and it contains two parts respectively at the HV and LV side, namely, V_{x1} and V_{x2} shown in Figure 3(a). V_h and V_l are the potential difference from the bottom tip of the HV sphere to point m, and that from point m to the upper tip of the grounded sphere.

$$\begin{cases} V_x = \int_{E \geq E_x} E dl \approx \sum_{E_k \geq E_x} E_k d_k \\ V_h = \int_{0 \leq l \leq L_{min}} E dl \approx \sum_{i=1}^{m} E_i d_k \\ V_l = \int_{L_{min} \leq l \leq d} E dl \approx \sum_{j=m+1}^{n} E_j d_k \end{cases} \tag{5}$$

(5) Path length, including L_{min} from the bottom tip of the HV sphere to point m, and the length of the line segment on which $E > E_x$, $E_g > E_g x = x\%E_{ghm}$, and the sum of $E_k^2 d_k$ equals to $x\%E_s$, respectively denoted as $L_E x$, $L_g x$ and $L_s x$.

TABLE 1. EF feature set for structural characterization of sphere gaps.

Category	Features	Number
Electric field strength	E_{hmax}, E_{lmax}, E_{min}, E_{a}, E_{std2}, E_{std}	6
Electric field gradient	E_{ghm}, E_{glm}, E_{ga}	3
Electric field square	E_{s}, E_{sa}	2
Electric field integral	V_{90}, V_{75}, V_{h}, V_{l}	4
Path length	L_{min}, L_{E90}, L_{E75}; L_{g90}, L_{g75}; L_{s90}, L_{s75}	7
Electric field inhomogeneity	E_{rha}, E_{rlh}, E_{rmh}; E_{rs90}, E_{rs75}; V_{r90}, V_{r75}, V_{rh}, V_{rl}; L_{rmin}, L_{rE90}, L_{rE75}, L_{rg90}, L_{rg75}, L_{rs90}, L_{rs75}	16

These features can be calculated by (6) and they are shown in Figure 3.

$$L_x = \sum_{k=1}^{p} d_k \tag{6}$$

(6) EF inhomogeneity, including several proportional quantities that are relevant to the above-mentioned features. This kind of features are defined as (7) – (10). In (9), U is the applied voltage between two sphere electrodes.

$$\begin{cases} E_{\mathrm{rha}} = E_{\mathrm{hmax}}/E_{\mathrm{a}} \\ E_{\mathrm{rlh}} = E_{\mathrm{l\,max}}/E_{\mathrm{h\,max}} \\ E_{\mathrm{rmh}} = E_{\mathrm{min}}/E_{\mathrm{h\,max}} \end{cases} \tag{7}$$

$$E_{\mathrm{rs}x} = \frac{\sum\limits_{E_k \geq E_x} E_k^2 d_k}{E_{\mathrm{s}}} \tag{8}$$

$$\begin{cases} V_{\mathrm{r}x} = V_x/U \\ V_{\mathrm{rh}} = V_{\mathrm{h}}/U \\ V_{\mathrm{rl}} = V_{\mathrm{g}}/U \end{cases} \tag{9}$$

$$L_{\mathrm{r}x} = L_x/d \tag{10}$$

In this paper, the ratio $x\%$ includes 90% and 75%. The above 38 features in total can be listed in Table 1. These features describe the EF distribution from different perspectives, thus to parameterize the sphere gap structure by some mathematical quantities.

III. SVC PREDICTION MODEL WITH PARTICLE SWARM OPTIMIZATION

An intelligent prediction model established by SVC was used for sphere gap breakdown voltage prediction. The input variables are the above-mentioned EF features, and the output parameters are two binary-class values, namely, -1 and 1. According to the output value, it can be judged whether gap breakdown occurs when it is submitted to a given voltage, thus to obtain the critical breakdown voltage. In this section, the SVC with particle swarm optimization (PSO) and the prediction procedure will be introduced.

A. SUPPORT VECTOR CLASSIFIER

For the investigated problems in this paper, we hope to predict as many air gap breakdown voltages as possible by machine learning of some limited training samples. It is actually a small-sample learning problem.

SVC is a machine learning algorithm used to solve binary classification problems. Compared with the traditional ANN-based approaches, it has unique advantages to deal with small-sample learning problems. The principle of SVC method is to map the original linearly inseparable data to a high-dimensional space via an appropriate kernel function. As shown in (11), the variable $\boldsymbol{x}$ in the Euclidean space $\mathbf{R}^n$ is converted to $\Phi(\boldsymbol{x})$ in the Hilbert space.

$$\mathbf{R}^n \rightarrow \text{Hilbert}, \quad \boldsymbol{x} \rightarrow \Phi(\boldsymbol{x}) \tag{11}$$

The method to deduce the decision function of the SVC can be viewed to construct and solve a nonlinear programming problem that is dual with the original classification problem. In the feature space, an optimal separating hyperplane with the maximum margin can be determined to classify the training sample data into two categories.

Details about the SVC theories are provided in [19], [20]. The LIBSVM toolbox [21] based on Matlab software was used for programming of the SVC model in this paper. The following radial basis function (RBF) kernel was used for feature mapping.

$$K(x_i, x_j) = \exp(-\gamma \left\| x_i - x_j \right\|^2), \quad \gamma > 0 \tag{12}$$

The SVC generalization performance is affected by two parameters. One is the penalty coefficient C and the other is the kernel parameter γ in (12). C describes the compromise between the maximum margin width and the minimum error in classification [20]. These two parameters should be properly optimized by some algorithms to minimize the prediction error. In this paper, they are automatically searched by the PSO algorithm.

B. PARTICLE SWARM OPTIMIZATION

PSO is a stochastic optimization algorithm based on swarm intelligence theory, which was introduced by Kennedy and Eberhart in 1995 [22]. PSO was inspired by the intelligent behaviors of bird flocking, and it has good global search capability. In the PSO algorithm, the solution of an optimization problem is viewed as a ''particle''. In an n-dimensional search space, m particles constitute a ''swarm''. Each particle has the properties of position, velocity and fitness value. Each particle flies in the n-dimensional solution space with its own velocity, and adjusts the velocity and position dynamically according to its flying experience and those of the other m-1 particles in the swarm.

For a swarm consists of m particles, each particle P_i $(i = 1, 2, \ldots, m)$ can be characterized by its current position $p_i(j) \in \mathbf{R}^n$, its velocity $v_i(j) \in \mathbf{R}^n$, and the best position $p_{\mathrm{b}i}(j) \in \mathbf{R}^n$ during its past flying trajectory, also called the individual extremum. Set $p_{\mathrm{gb}i}(j) \in \mathbf{R}^n$ as the global best position, that is, the global extremum, searched by all the particles in the swarm. The particle will update its velocity and position according to (13), and therefore it will gradually

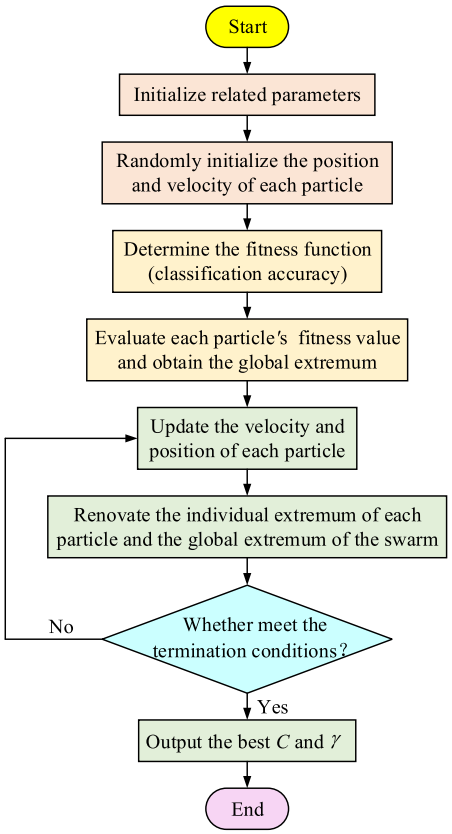

FIGURE 4. Flow chart of PSO algorithm.

fly to the optimal position.

$$\begin{cases} v_i(j+1) = wv_i(j) + c_1 r_1(j)[p_{\mathrm{b}i}(j) - p_i(j)] \\ \qquad\qquad + c_2 r_2(j)[p_{\mathrm{gb}i}(j) - p_i(j)] \\ p_i(j+1) = p_i(j) + v_i(j+1) \end{cases} \tag{13}$$

where w is the inertial weight, c_1 and c_2 are two acceleration constants, also called the learning factors, $r_1(j)$ and $r_2(j)$ are two random variables generated from 0 to 1. It can be seen that the particle velocity is composed of three parts. The first one is the memory term reflecting the current status of the particle, the second one is the cognition term representing the self-learning of its own experience to get enough strong global search ability, and the third one is the social term characterizing the cooperation and information sharing between different particles.

The flow chart of PSO algorithm is shown in Figure 4, and the process is introduced as follows:

1) Initialize the size of the particle swarm, the maximum number of iterations, and the related parameters including the inertial weight w, the learning factors c_1 and c_2.

2) Initialize the position and velocity of each particle randomly in the search space and calculate the fitness value of each particle. In this paper, the SVC classification accuracy of the training samples in the case of K-fold cross validation (K-CV) is taken as the fitness function. The individual extremum of each particle and the global extremum of the swarm are recorded.

3) Update the velocity and position of each particle according to (13), calculate the fitness value of each particle, and renovate the individual extremum of each particle and the global extremum of the swarm.

4) Check the termination conditions to judge whether to stop searching or not. If the stopping criterion is satisfied, the algorithm is terminated and the optimal parameters are output. Otherwise, return to step 3) and continue iterations.

C. PREDICTION PROCEDURE

The implementation process of the breakdown voltage prediction by PSO-optimized SVC model is depicted in the following steps:

Step 1: Feature data pre-processing

The EF feature set contains various parameters, some are with physical significance, and some are only mathematical quantities. These features are of different units and orders of magnitudes. In order to avoid the effects on the prediction, the input feature data are normalized to the range [0, 1] by

$$x_i^* = \frac{x_i - x_{i\min}}{x_{i\max} - x_{i\min}} \tag{14}$$

where x_i^* is the normalized value of the variable x_i, $x_{i\max}$ and $x_{i\min}$ are the maximum and minimum values, respectively.

Step 2: SVC parameter optimization by PSO

According to the above introduction, SVC parameter optimization process by PSO algorithm can be summarized as parameter initialization, fitness evaluation, adjustment and update of particles' properties, and termination checking. The K-CV is applied to judge the classification capability of the SVC model under the found parameters. The training data are divided into K sets. Each subset is taken as the validation set for one time, while the other K-1 sets are training sets. For a parameter group (C, γ) found by PSO during the iterations, the average value of the classification accuracy for the K times of testing is the index for SVC performance evaluation. The values of the penalty coefficient C and the kernel parameter γ are updated constantly until the maximum number of iterations has been reached, then the algorithm is terminated. The parameters with the highest classification accuracy are taken as the optimization results.

Step 3: Model training and breakdown voltage prediction

Under the optimal parameters searched by PSO, the trained SVC model is applied for breakdown voltage prediction of test samples. The EF features are input to the model, which are calculated under different applied voltages generated by the golden section search method [23]. The applied voltage is updated continuously according to the SVC output, namely, -1 or 1, and iterative predictions are carried out until the critical value is determined, and it is the predicted result of the breakdown voltage. This process has been described in detail in the previous study [23].

Three commonly used error indexes, namely, RMSE, MAPE and MSPE were used to evaluate the performance of

TABLE 2. Investigated sphere gaps and the sample size of each f interval.

Sphere gaps		Electric field nonuniform coefficient	
D (cm)	d (cm)	f interval	Sample size
5	1.0~2.4	(1, 1.05]	58
6.25	1.0~3.0	(1.05, 1.1]	57
10	1.0~5.0	(1.1, 1.15]	41
12.5	1.0~6.0	(1.15, 1.2]	23
15	1.0~7.5	(1.2, 1.25]	19
25	1.0~12	(1.25, 1.3]	18
50	2.0~24	(1.3, 1.35]	15
75	2.0~36	(1.35, 1.4]	13
100	3.0~50	(1.4, 1.45]	9
150	5.0~75	(1.45, 1.5]	7
200	10~100	(1.5, 1.55]	11

TABLE 3. Five groups of randomly selected training set.

Set 1		Set 2		Set 3		Set 4		Set 5	
D	d	D	d	D	d	D	d	D	d
5	1.4	5	2.2	5	1.6	5	1.5	6.25	3
5	2.2	6.25	3.0	10	2.0	12.5	5.0	10	1.6
10	4.5	12.5	1.4	15	7.0	15	3.5	10	2.8
15	6.0	12.5	2.8	25	10	25	2.2	10	3.0
25	5.5	12.5	5.0	25	12	50	24	10	3.5
25	8.0	25	1.5	50	13	75	32	15	6
50	8.0	50	17	100	24	100	4.0	25	11
50	17	75	19	100	36	100	17	75	5.5
75	5.5	150	45	150	7.5	100	45	100	14
75	10	200	38	150	20	150	38	150	36
200	100	200	90	150	65	200	70	150	70

*The units of D and d are both cm.

the prediction model. They are calculated by

$$\begin{cases} \text{RMSE} = \sqrt{\dfrac{1}{n}\displaystyle\sum_{i=1}^{n}(U_{ei} - U_{pi})^2} \\ \text{MAPE} = \dfrac{1}{n}\displaystyle\sum_{i=1}^{n}\left|U_{ei} - U_{pi}\right|/U_{ei} \\ \text{MSPE} = \dfrac{1}{n}\sqrt{\displaystyle\sum_{i=1}^{n}[(U_{ei} - U_{pi})/U_{ei}]^2} \end{cases} \tag{15}$$

where U_{ei} and U_{pi} are the experimental and predicted breakdown voltage of the ith test sample, respectively, and n is the test sample size.

In this study, all of the above-mentioned approaches and algorithms were coded in Matlab software. The predictions were conducted automatically.

IV. SPHERE GAP BREAKDOWN VOLTAGE PREDICTION

The SVC model was employed for breakdown voltage prediction of sphere gaps with different diameters and a wide range of gap spacings. The sample data were collected from IEC 60052 [18], which provides the standard peak values of the power frequency breakdown voltage of sphere gaps used for voltage measurement. These experimental values were taken for comparisons with the predicted results, thus to demonstrate the effectiveness of the proposed EF feature set and the prediction model.

A. SAMPLE SELECTION

The investigated sphere gaps are summarized in the left half part of Table 2, with 271 sample data in total, while the training and test samples are selected from them.

Air gap breakdown voltage has a close relation with the EF inhomogeneity. The EF nonuniform coefficient, denoted as f, is defined as

$$f = \frac{E_{\max}}{U/d} \tag{16}$$

where $E_{\max}$ is the maximum EF intensity under the applied voltage U. The value of $E_{\max}$ is calculated by FEM, and thus to further calculate the value of f.

In this paper, the samples for SVC model training were selected according to f intervals. According to the FEM calculation results, the values of f for the 271 sphere gaps range from 1 to 1.55, which are all with quasi-uniform electric field. The f values for different sphere gaps can be divided into 11 ranges with a step size of 0.05. The number of the sphere gaps belong to each f value range are shown in the right half part of Table 2, which divides the 271 samples into 11 groups. To ensure the training effect of the SVC model and guarantee its generalization ability, one sample was randomly selected from each group to constitute the training sample set. Therefore, 11 samples were applied for model training and the test samples are the other 260 sphere gaps.

Since the training samples were selected randomly, five repetitive predictions based on different training samples were conducted to verify the prediction accuracy. The five groups of training sample set are listed in Table 3.

B. RESULTS AND DISCUSSIONS

The PSO algorithm based on 3-CV was implemented to search the optimal SVC parameters C and γ for each group of training sample set. The maximum number of iterations is 200, and the initial population size of swarm is set as 30. The inertia weight $w = 1$ and the learning factors $c_1 = 1.5$, $c_2 = 1.7$. The search ranges of C and γ are [0, 500] and [0.005, 0.25]. The parameter optimization process under training set 2 is shown in Figure 5. The optimal parameters are $C = 82.7873$, $\gamma = 0.02947$, and the SVC model has the best CV accuracy 97.4026% for training set 2. Similarly, the optimal C and γ can also be found by PSO for the other 4 groups of training sample set. The trained SVC models after parameter optimization were applied for breakdown voltage prediction of the 260 test samples, and a comparison between the predicted results and the experimental data provided in IEC 60052 [18] was carried out for error analysis.

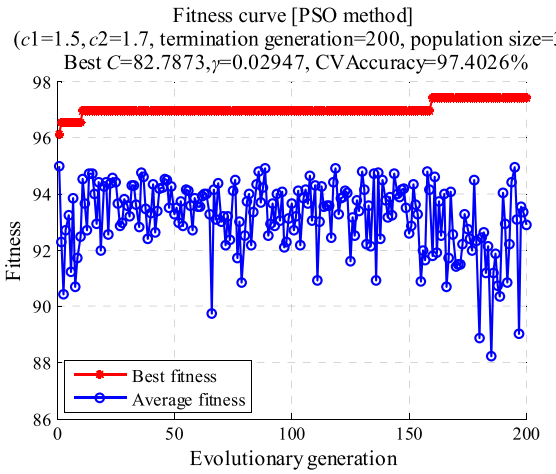

FIGURE 5. Parameter optimization process of PSO algorithm.

TABLE 4. Optimal parameters and error indexes of the five predictions.

Results	Set 1	Set 2	Set 3	Set 4	Set 5
C	90.5637	82.7873	15.2112	89.7086	48.2906
γ	0.01713	0.02947	0.05573	0.01766	0.02691
RMSE	16.690	8.085	9.276	10.250	6.559
MAPE	0.0188	0.0200	0.0141	0.0137	0.0143
MSPE	0.0015	0.0015	0.0012	0.0011	0.0012

For the 5 predictions with different training sample sets, the optimal parameters and the prediction errors are summarized in Table 4. As listed in Table 4, the three error indexes are very small, while the MAPEs are 1.88%, 2.00%, 1.41%, 1.37% and 1.43% for the five predictions based on different training sample sets, which were selected randomly according to the f value range. The predicted results have high accuracy, which means that the PSO-optimized SVC model has strong learning ability and generalization performance under the circumstances of small samples.

For better comparisons, taking the results based on training set 2 as an example, the breakdown voltage values for sphere gaps with different structure sizes are plotted together in Figure 6. It can be observed that the predicted U-d curves are very close to the experimental ones, with the same trend and minor relative errors. With the input variables of the proposed EF features, and trained by a small sample set with only 11 data, the proposed PSO-optimized SVC model realizes breakdown voltage prediction of 260 sphere gaps with excellent accuracy.

In order to further prove the validity of this prediction method, the PSO-optimized SVC model, respectively trained by the above five groups of training set, was used to predict the power frequency breakdown voltages of sphere gaps with different diameters. The breakdown tests were carried out to measure the experimental breakdown voltage values for comparison with the predicted results. As shown in Figure 7, the large sphere diameter is 9.75 cm and it was applied high voltage; the small sphere diameter is 6.5 cm and it was grounded. The experimental results (peak values) were corrected to standard atmospheric condition, which were shown in Table 5 as U_t. The predicted results with five training sets are shown in Table 5, respectively denoted as U_{p1} to U_{p5}. It can be seen that the MAPEs of the five groups of prediction results are within 2.6%. Also, taking the results with training set 2 for example, the comparison between the

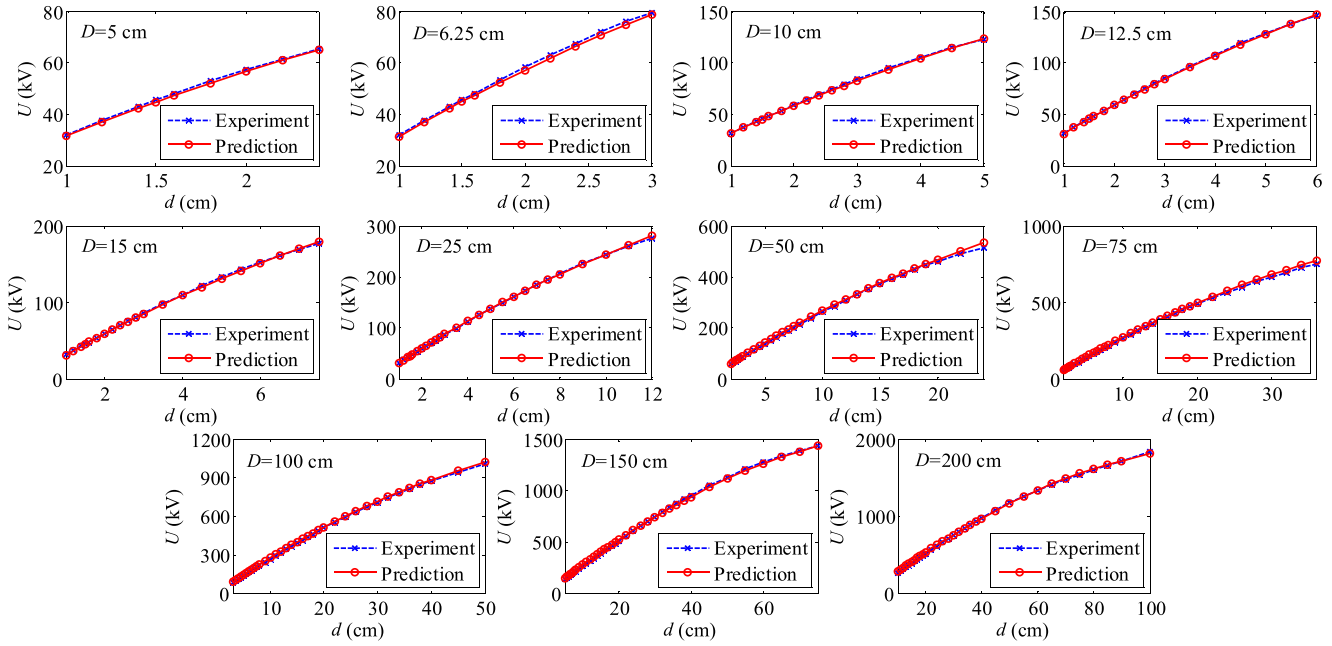

FIGURE 6. Sphere gap breakdown voltage prediction results by PSO-optimized SVC model with training set 2.

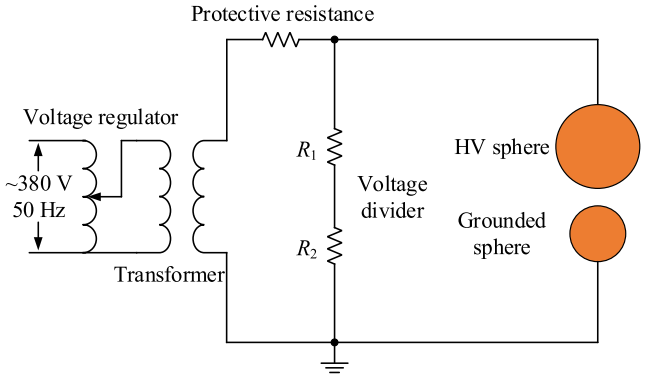

FIGURE 7. Schematic diagram of Φ9.75 cm sphere – Φ6.5 cm sphere gap breakdown test with power frequency AC voltage.

TABLE 5. Breakdown voltage prediction results of Φ9.75 cm sphere – Φ 6.5 cm sphere gaps with different training sets.

d (cm)	U_t (kV)	U_{p1} (kV)	U_{p2} (kV)	U_{p3} (kV)	U_{p4} (kV)	U_{p5} (kV)
1.0	30.5	30.2	31.5	30.1	30.7	30.1
1.5	44.6	44.4	46.2	44.6	44.5	44.5
2.0	58.7	57.9	60.3	58.4	57.6	58.4
5.5	71.8	70.7	73.7	71.6	70.0	72.1
3.0	84.3	82.5	86.5	83.9	82.2	84.2
3.5	96.0	93.3	98.0	95.2	93.6	94.7
4.0	106.8	103.6	108.0	105.3	104.1	104.6
MAPE	—	0.0175	0.0258	0.0069	0.0183	0.0086

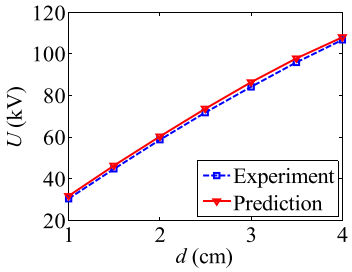

FIGURE 8. Φ9.75 cm sphere–Φ6.5 cm sphere gap breakdown voltage prediction results by PSO-optimized SVC model with training set 2.

predicted and experimental breakdown voltages of Φ9.75 cm sphere – Φ6.5 cm sphere gaps is shown in Figure 8. The U-d curves coincide well with small errors. It can be drawn from the prediction results that the proposed PSO-optimized SVC model is also effective to predict the breakdown voltages of other similar gap structures. This study is significant to promote the realization of air insulation strength prediction by mathematical approaches.

Previous experimental and theoretical studies on air discharge have lasted for over a century, which contributes to better understanding about the fundamental scientific mechanisms of this phenomenon. However, due to the limitations of the imperfect discharge theories, the insulation design of electrical equipment still relies on empirical conclusions, i.e., the correlations between the discharge voltage and the gap spacing for various configurations. It can be concluded that a rigorous theoretical calculation of air gap strength needs further studies, while empirical fitting formulas are usually with limited applicability. On this background, the idea proposed in this paper provides an alternative to solve this problem, with the combination of EF calculation, feature extraction and SVC prediction. The key scientific problems of this innovative approach are how to parameterize the influencing factors of air dielectric strength, and how to realize reasonable modeling of their relationships. The studies presented in this paper make a step forward on this assumption, and the satisfactory prediction results have preliminarily verified the feasibility of this method.

It should be noted that further studies are still necessary to improve this model and promote this approach to other gap configurations. The feature set defined in this paper has been applied for sphere gap breakdown voltage prediction, which may be applicable for those gap structures that have similar interelectrode EF distributions, such as the ring-ring gaps. However, for other gap types, such as rod-plane gaps, and those real-world gaps with complex electrode structures and severe nonuniform electric field, the feature set should be redefined according to the structural characteristics. In addition, some feature selection methods will be used to simplify the EF feature set. On the other hand, data collection of air gaps with various configurations is also an important task in future work. We think the combination of big data and machine learning algorithms is hopeful to bring some interesting conclusions on this research domain, which will be an underlying focus of future investigations.

V. CONCLUSION

This paper presents a feature set used for structural characterization of the sphere gap, and proposes a machine learning model based on PSO-optimized SVC for breakdown voltage prediction.

1) The EF feature set extracted along the sphere gap interelectrode path is effective to characterize its electrostatic field distribution, and these features can be used as input parameters of the PSO-optimized SVC model for sphere gap breakdown voltage prediction with a wide range of sphere diameters and gap spacings.

2) Reasonable selection of training sample set in terms of the EF nonuniform coefficient is helpful to ensure the generalization performance of the PSO-optimized SVC model in the case of small samples. Trained by only 11 randomly selected training samples, the SVC model predicts the breakdown voltages of 260 sphere gaps, while the MAPE is within 2.0% compared with the IEC 60052 standard values. A prediction case carried out on Φ9.75 cm sphere – Φ6.5 cm sphere gaps also has high accuracy.

3) This study offers an alternative to acquire air insulation strength instead of theoretical calculation based on the physical mechanism and empirical fitting according to the experimental results, which is beneficial to guide insulation design of electrical equipment in the future.

REFERENCES

[1] J. S. Townsend, *The Theory of Ionization of Gases by Collision*. New York, NY, USA: Van Nostrand, 1910.
[2] H. Reather, *Electron Avalanches and Breakdown in Gases*. London, U.K.: Butterworths, 1964.
[3] L. B. Loeb and J. M. Meek, *The Mechanism of the Electric Spark*. Redwood City, CA, USA: Stanford Univ. Press, 1941.
[4] J. J. Lowke and F. D'Alessandro, "Onset corona fields and electrical breakdown criteria," *J. Phys. D, Appl. Phys.*, vol. 36, no. 21, pp. 2673–2682, Oct. 2003.
[5] F. W. Peek, *Dielectric Phenomena in High Voltage Engineering*. New York, NY, USA: McGraw-Hill, 1929.
[6] M. Abdel-Salam and N. L. Allen, "Inception of corona and rate of rise of voltage in diverging electric fields," *Proc. A Phys. Sci., Meas. Instrum., Manage. Educ.*, vol. 137, no. 4, pp. 217–220, Jul. 1990.
[7] Y. Chen, Y. Zheng, and X. Miao, "Breakdown conditions of short air-insulated gaps under alternating non-uniform electric fields," *J. Appl. Phys.*, vol. 122, no. 3, Jul. 2017, Art. no. 033304.
[8] L. Thione, A. Pigini, N. L. Allen, M. Aro, and A. Baker, "Guidelines for the evaluation of the dielectric strength of external insulation," in *Proc. Int. Council Large Electr. Syst. (CIGRE)*, Paris, France, vol. 72, 1992, pp. 29–42.
[9] A. Beroual and I. Fofana, *Discharge in Long Air Gaps: Modelling and Applications*. Bristol, U.K.: IOP, 2016, pp. 1–7.
[10] Z. B. Qiu, J. Ruan, D. Huang, Z. Pu, and S. Shu, "A prediction method for breakdown voltage of typical air gaps based on electric field features and support vector machine," *IEEE Trans. Dielectr. Elect. Insul.*, vol. 22, no. 4, pp. 2125–2135, Aug. 2015.
[11] L. Mokhnache, A. Boubakeur, and A. Feliachi, "Breakdown voltage prediction in a point-barrier-plane air gap arrangement using self-organization neural networks," in *Proc. IEEE Power Eng. Soc. General Meeting*, Denver, CO, USA, Jun. 2004, pp. 569–572.
[12] M. T. Gençoğlu and M. Cebeci, "Investigation of pollution flashover on high voltage insulators using artificial neural network," *Expert Syst. Appl.*, vol. 36, no. 4, pp. 7338–7345, May 2009.
[13] S. A. Bessedik and H. Hadi, "Prediction of flashover voltage of insulators using least squares support vector machine with particle swarm optimisation," *Electr. Power Syst. Res.*, vol. 104, pp. 87–92, Nov. 2013.
[14] Z. Qiu, J. Ruan, D. Huang, M. Wei, L. Tang, C. Huang, W. Xu, and S. Shu, "Hybrid prediction of the power frequency breakdown voltage of short air gaps based on orthogonal design and support vector machine," *IEEE Trans. Dielectr. Electr. Insul.*, vol. 23, no. 2, pp. 795–805, Apr. 2016.
[15] Z. Qiu, J. Ruan, C. Huang, W. Xu, L. Tang, D. Huang, and Y. Liao, "A method for breakdown voltage prediction of short air gaps with atypical electrodes," *IEEE Trans. Dielectr. Elect. Insul.*, vol. 23, no. 5, pp. 2685–2694, Oct. 2016.
[16] Y. Bourek, L. Mokhnache, N. N. Said, and R. Kattan, "Study of discharge in point-plane air interval using fuzzy logic," *J. Electr. Eng. Technol.*, vol. 4, no. 3, pp. 410–417, Sep. 2009.
[17] G. E. Asimakopoulou, V. T. Kontargyri, G. J. Tsekouras, N. Ch Elias, F. E. Asimakopoulou, and I. A. Stathopulos, "A fuzzy logic optimization methodology for the estimation of the critical flashover voltage on insulators," *Electr. Power Syst. Res.*, vol. 81, no. 2, pp. 580–588, Feb. 2011.
[18] *Voltage Measurement by Means of Standard air Gaps*, Standards IEC 60052, 2002.
[19] V. N. Vapnik, *The Nature of Statistical Learning Theory*, 2nd ed. New York, NY, USA: Springer, 2000, pp. 131–170.
[20] S. Abe, *Support Vector Machines for Pattern Classification*, 2nd ed. London, U.K.: Springer, 2010, pp. 21–112.
[21] C.-C. Chang and C.-J. Lin, "LIBSVM: A library for support vector machines," *ACM Trans. Intel. Syst. Technol.*, vol. 2, no. 3, p. 27, Apr. 2011.
[22] J. Kennedy and R. Eberhart, "Particle swarm optimization," in *Proc. IEEE Int. Conf. Neural Netw.*, Perth, WA, Australia, 1995, pp. 1942–1948.
[23] Z. B. Qiu, J. Ruan, W. Xu, and C. Huang, "Energy storage features and a predictive model for switching impulse flashover voltages of long air gaps," *IEEE Trans. Dielectr. Electr. Insul.*, vol. 24, no. 5, pp. 2703–2711, Oct. 2017.

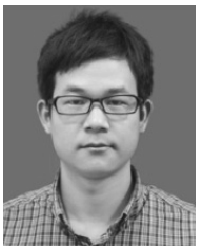

ZHIBIN QIU (M'18) was born in Jiangxi, China, in 1991. He received the B.S. degree in electrical engineering and automation and the Ph.D. degree in high voltage and insulation technology from the School of Electrical Engineering, Wuhan University, Wuhan, China, in 2011 and 2016, respectively, where he was involved in a Postdoctoral Research, from 2016 to 2018. He is currently a Distinguished Professor with the Department of Energy and Electrical Engineering, Nanchang University, Nanchang, China. His research interests include air gap discharge characteristics, the external insulation of transmission and transformation equipments, and the fault diagnosis of electrical equipments.

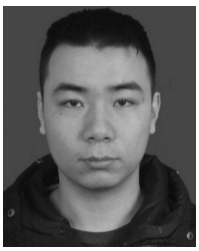

XUEZONG WANG was born in Hubei, China, in 1994. He received the B.S. degree in electrical engineering and automation from the School of Electrical Engineering, Wuhan University, Wuhan, China, in 2016, where he is currently pursuing the Ph.D. degree in electrical engineering. His research interests include electromagnetic field simulation, high voltage, and insulation technology.